

Computer simulations of phase equilibrium for a fluid confined in a disordered porous structure

L. Sarkisov and P. A. Monson*

Department of Chemical Engineering, University of Massachusetts, Amherst, Massachusetts 01003

(Received 27 January 2000)

We present calculations of the phase diagrams of a Lennard-Jones 12-6 fluid confined in a disordered porous structure made up of a dispersion of spherical particles, following up on an earlier work on the same system. In particular we present additional calculations using more realizations of the matrix and we investigate the applicability of the Gibbs-Duhem integration method to the calculation of phase equilibrium in these systems. The essential picture of disordered and inhomogeneous coexisting vapor and liquid phases, which emerged in the earlier work, is confirmed by the new calculations. However, a second phase transition associated with the wetting of the porous material by the fluid is found to be more sensitive to variations of the matrix realization. While for the present model this transition appears for particular realizations of the matrix, it does not seem to survive averaging over realizations.

PACS number(s): 61.20.Gy, 05.70.Fh, 64.60.Fr

The behavior of fluids confined in disordered porous materials has been the subject of intense experimental [1,2] and theoretical [3–5] interest over the last several years. A key issue in developing an understanding of the behavior of such systems is to determine the coupled roles of porous material disorder, confinement, and wetting phenomena.

One of the most promising theoretical approaches to these systems has emerged from studies of molecular models that treat a disordered porous material, such as a silica gel, as a collection of particles arranged in a predetermined microstructure [7,8]. Such models are amenable to study by statistical mechanical theories using cluster expansion and replica techniques [5,6] as well as by computer simulation [7–13].

In recent work [9], a Monte Carlo simulation study of a model of a fluid confined in a silica xerogel was presented in which the vapor-liquid coexistence was estimated using thermodynamic integration techniques. Several conclusions emerged from that work. In addition to the suppression of the critical temperature associated with confinement, the shape of the coexistence curve was found to reflect both the wetting behavior of the fluid in the porous material and the disorder. The results suggested an additional phase transition that was associated with the ability of the fluid to wet the more dense regions of the porous material (such a transition is predicted for several model systems in the context of theories based on the replica Ornstein-Zernike equation [6]). The effect of disorder was assessed through the comparison of the adsorption isotherms calculated for a disordered configuration of solid particles, which was obtained from an equilibrium hard-sphere Monte Carlo simulation with those for a fluid confined in an ordered array (fcc) of solid particles. The purpose of this paper is to follow up on this earlier work with additional investigations of some issues. In particular we make a wider study of the dependence of the results on the number of realizations of the porous matrix considered and we investigate the utility of the Gibbs-Duhem integration method [14] for determining the phase coexistence in these systems more efficiently.

In this work we use one of the two molecular models considered most extensively by Page and Monson [9]. We model the solid as an array of spherical particles in a configuration (realization) taken from a Monte Carlo simulation of an equilibrium hard-sphere system. We use the composite sphere potential developed by Kaminsky and Monson [8] to model the fluid-solid interactions, as adapted to study changes in the strength of the fluid-solid attractions [9]. For the ratio of solid-fluid to fluid-fluid well depths we use $\epsilon_{sf}/\epsilon_{ff}=1.144$. The fluid-fluid potential was truncated at $2.5\sigma_{ff}$ and the solid-fluid potential at $8.08\sigma_{sf}$. The solid volume fraction was set to 0.386 and the size ratio between the matrix spheres and fluid molecules is 7.055:1. All the calculations were carried out with the grand canonical Monte Carlo technique [15] using 32 matrix particles and cell lists to reduce the computer time required for summing the interactions in the system. The simulations were typically run for over 10^8 configurations with half of these used for equilibration.

We have made calculations of phase diagrams using both thermodynamic integration, as described in the work of Page and Monson [9], and the Gibbs-Duhem integration technique [14]. The main drawback of thermodynamic integration is that it requires a complete adsorption/desorption isotherm for each temperature on the phase diagram. Gibbs-Duhem integration [14] offers a potentially more efficient technique and has been recently extended to the grand ensemble [16]. Another alternative has been considered by Alvarez *et al.* [12] and Escobedo and de Pablo [13] who have used histogram reweighting [17] in their recent studies. This method is not so convenient in the present case because the very large number of particles in the simulations at high density make the distribution functions in our grand ensemble simulations extremely narrow. In the Gibbs-Duhem integration method we propagate the chemical potential of the phases in coexistence along the saturation line by integrating the expression [16]

$$\left(\frac{d\mu}{dT}\right) = -\frac{\Delta(\rho U)}{T\Delta\rho} + \frac{\mu}{T}, \quad (1)$$

*Author to whom correspondence should be addressed.

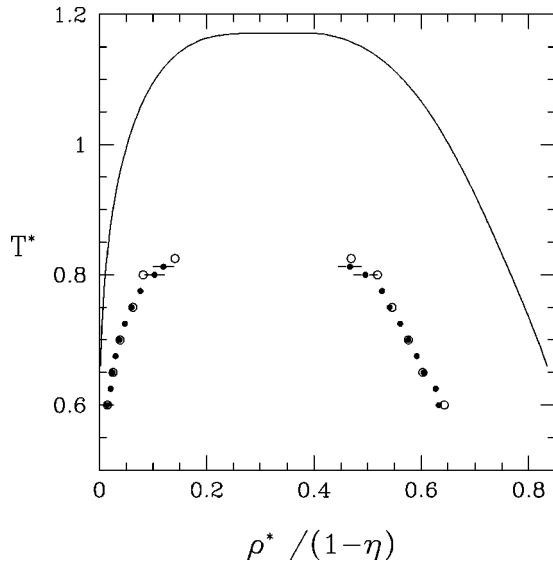


FIG. 1. Temperature kT/ϵ_{ff} vs density $\rho\sigma_{ff}^3/(1-\eta)$ (where η is the volume fraction of the hard-sphere matrix) coexistence curves for 12-6 fluid confined in an ordered fcc matrix calculated via thermodynamic integration (open circles) and via Gibbs-Duhem integration (closed circles) compared with that of the bulk fluid (line).

where Δ in front of a quantity denotes a difference in that property between the two phases and it is understood that the derivative is being evaluated along the coexistence curve. This equation has the form of an ordinary differential equation and can be integrated to give $\mu_{coex}=f(T)$. The choice of integrator is influenced by the need to minimize the number of evaluations on the right-hand side of Eq. (1), since this requires a computer simulation of each coexisting phase. For this reason predictor-corrector techniques have an advantage over Runge-Kutta and some other more sophisticated methods. We use the third order Adams-Bashforth predictor-corrector scheme [18], which is a reasonable compromise between simplicity and stability properties. For the start up of this scheme we need the first three values of $(d\mu/dT)$ (we call this a start up set), which requires an independent calculation of the coexistence properties using thermodynamic integration. Nevertheless, the Gibbs-Duhem integration method is still potentially much less time consuming than thermodynamic integration.

We have tested the Gibbs-Duhem approach for two cases: the ordered fcc matrix and a single realization of the disordered matrix. In Fig. 1 we compare phase diagrams calculated via Gibbs-Duhem integration with those obtained via thermodynamic integration [11] for the fluid confined in the fcc matrix. In this figure the bulk vapor-liquid coexistence curve, corrected for the effect of truncating the potential, is also shown. This was calculated from the accurate equation of state of Johnson *et al.* [19]. For the Gibbs-Duhem integration we used a temperature interval $\Delta T^*=0.025$ (where $T^*=kT/\epsilon_{ff}$) with the start up set, $T^*=0.6, 0.625, \text{ and } 0.65$ (for the highest temperature shown we restarted the Gibbs-Duhem integration with $\Delta T^*=0.0125$ and a start up set $T^*=0.775, 0.7875$ and 0.8 with the values at the middle temperature obtained by interpolation). We see that there is very good agreement between the two methods for calculating the phase coexistence. Notice that for this ordered matrix

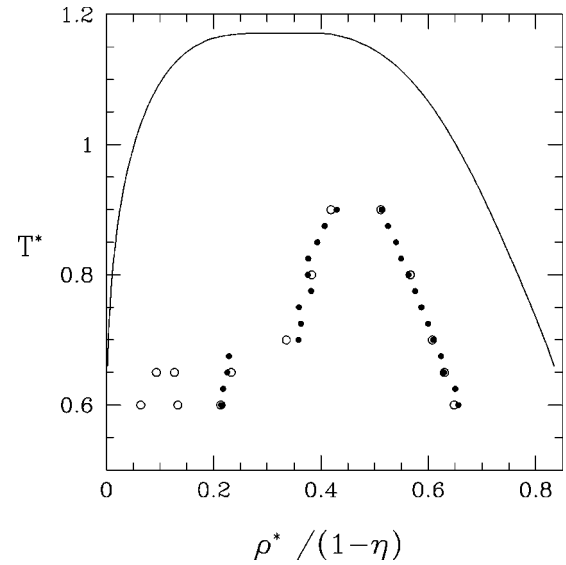


FIG. 2. Temperature kT/ϵ_{ff} vs density $\rho\sigma_{ff}^3/(1-\eta)$ phase diagrams for 12-6 fluid confined in a single realization of the disordered matrix calculated via thermodynamic integration (open circles) and via Gibbs-Duhem integration (closed circles) compared with that of a bulk fluid (line).

the shape of the coexistence curve for the confined fluid is very similar to that of the bulk fluid although the critical temperature is substantially lowered by confinement [11].

In Fig. 2 the corresponding comparison is shown for the disordered matrix using the same realization considered in the earlier work [9]. The implementation of the Gibbs-Duhem integration turned out to be more problematic in this case. First of all we note that in the earlier results of Page and Monson [9] the phase diagram shows evidence of a second phase transition at the low density side of the main coexistence region. The coexistence points marked here were estimated simply on the basis of the jumps in the adsorption isotherms. To carry out the thermodynamic integration, the isotherms were integrated assuming that these jumps marked the equilibrium points, an assumption that does not significantly impact the accuracy of the calculated vapor-liquid coexistence properties. Thus for the Gibbs-Duhem integration we only attempted a calculation of the main coexistence region. As can be seen there is good agreement between the two calculation methods. However, to obtain this agreement we had to restart the integration from $T^*=0.70$ with the start up set $T^*=0.65, 0.675, \text{ and } 0.70$. At this point the phase diagram obtained via thermodynamic integration shows a significant increase in the coexisting vapor density. The Gibbs-Duhem integration would not have captured this effect if we had not restarted the integration with $T^*=0.7$ in the start up set. Gibbs-Duhem integration [14,16] has been successfully applied most often to systems with relatively smoothly changing coexistence densities as a function of temperature. A system like the present one requires additional tests of the phase behavior and a more sophisticated integration scheme with a smaller integration step, thereby reducing the effectiveness of the approach.

We now turn to the calculation of the phase diagram averaged over several different realizations of the porous material. We used only thermodynamic integration in this cal-

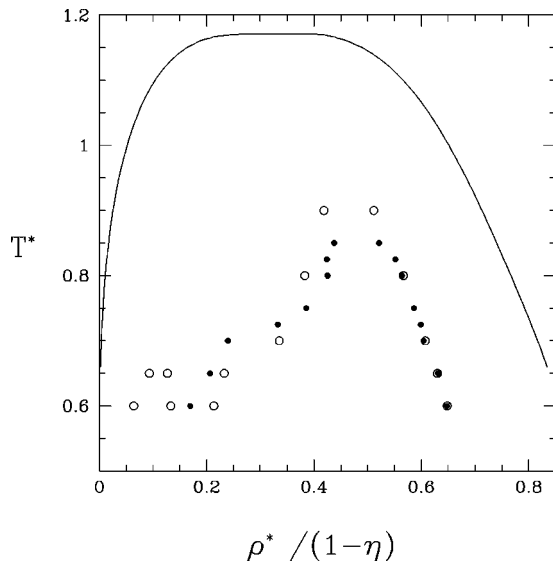


FIG. 3. Temperature kT/ϵ_{ff} vs density $\rho\sigma_{ff}^3/(1-\eta)$ phase diagrams for 12-6 fluid confined in a single realization of the disordered matrix (open circles) and for the multiple realizations (closed circles, ten realizations for $T^*=0.6$ and 0.65 , and five realizations for the rest of the points) compared with that of a bulk fluid (line).

ulation. Adsorption isotherms we calculated for each realization at every temperature point and then averaged over the realizations to produce a single average isotherm. This isotherm was then used in the thermodynamic integration procedure to calculate properties of the phases in coexistence. Thermodynamic integration requires knowledge of an initial grand potential density for a condensed fluid state outside the two-phase region. These values were estimated using a single matrix realization, since at high temperatures and high densities the properties of the confined fluid become relatively insensitive to changes in the matrix realization.

The results for the phase diagram calculated in this way are shown in Fig. 3 together with those for the single realization considered in the earlier work. Results at the lowest two temperatures ($T^*=0.6$ and $T^*=0.65$) were averaged over ten matrix realizations and those at the higher temperatures were averaged over five realizations. Again the coexistence curve for the bulk fluid is also shown. There are several things to notice about these results. First there is very good agreement for the liquid phase coexistence densities of the confined fluid between the single realization results and the realization averaged results. Also, while there are some quantitative differences, the vapor phase densities follow a similar trend in the two cases. A key feature here is the high density of the vapor phase relative to that in the bulk. This is due to the presence of relative high density fluid in the lower porosity regions of the matrix. This point is well illustrated by the computer graphics visualization in Fig. 14 of the second paper by Page and Monson [9] and qualitatively similar behavior is seen in visualizations for other matrix realizations. In both the single realization case and the averaged results we observe a significant narrowness of the phase diagram toward higher densities and a shoulder in the vapor densities in the temperature region between $T^*=0.65$ and $T^*=0.75$. On the other hand, averaging over several matrix realizations eliminates the apparent second transition shown

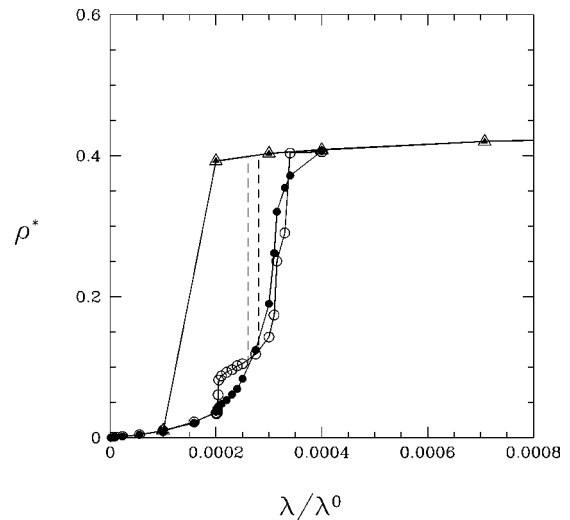


FIG. 4. Adsorption/desorption isotherms of density $\rho\sigma_{ff}^3$ vs relative activity λ/λ^0 at $kT/\epsilon_{ff}=0.6$ for the 12-6 fluid confined in a single realization of the disordered matrix (open circles and triangles for adsorption and desorption, respectively) and averaged over ten realizations (closed circles and triangles for adsorption and desorption, respectively). Dashed lines connect phases in coexistence for the single realization (right line) and for multiple realizations (left line). Here λ^0 is the activity at vapor-liquid coexistence for the bulk.

on the left side of the phase diagram for the single realization case. We have found steplike behavior in this region for some of the isotherms (as was the case for the two realizations looked at by Page and Monson [9]) but not others and there is some variation in the location of the step between different realizations.

It is also of interest to compare the averaged adsorption isotherms with those for a single realization and such a comparison is shown for $T^*=0.60$ in Fig. 4. It can be seen that the coexistence densities (connected with dashed lines) are similar for both the multiple and single realization isotherms. At the same time it is clear that the second transition seen for the single realization isotherm (at about $\lambda/\lambda^0=0.0002$) is not present for the averaged isotherm. On the other hand, there is very close agreement of the high density branches of the isotherms in the two cases.

Given this new information it is worthwhile to reflect briefly on the status of the second phase transition. The evidence for this transition in the single realization studied by Page and Monson [9] is quite convincing and has been confirmed for the case of the repulsive matrix that was also considered in that work by Escobedo and de Pablo [13] as well as for single realizations of models with equal sized solid and fluid particles [12,13]. The possibility of an additional phase transition arises because of the variation in porosity in the system leading to regions of low porosity that can span the sample. The second transition seen by Page and Monson [9] is associated with the filling of such a sample spanning region of low porosity. What appears to happen for the present model is that these sample spanning regions of low porosity are fragile to variations in matrix realization (whether this true for other size ratios is not clear). Of course a similar analysis applies to the main vapor-liquid transition. The existence of this transition requires the presence of a

region of high porosity, which is sample spanning. Our results indicate that for the present system the existence of such regions is robust to variations in the realization. Hysteresis between high and low density branches in the adsorption isotherms indicative of the vapor-liquid transition is seen for all the realizations we have studied. Moreover by varying the parameters in the model we can obtain hysteresis loops that bear a remarkable resemblance to those seen experimentally [11].

To summarize, we have presented some new results on the calculation of phase diagrams for a molecular model of a fluid confined in a disordered porous material. We have tested the applicability of the Gibbs-Duhem integration technique to this problem. With this technique we have been able to reproduce results obtained via thermodynamic integration. However the method works best when the coexistence densities are relatively smoothly varying functions of temperature (a feature that makes the solutions of the differential

equation more accurate for a given step size in temperature), which is not always the case in these systems. Phase diagram calculations were presented based on adsorption isotherms averaged over several realizations of the porous structure carried out via thermodynamic integration. Such features of the phase behavior as lowering of the critical temperature, narrowness of the coexistence region, and its shift toward higher densities that were seen in earlier results for a single realization [9] are preserved in the averaging over realizations. However, the second transition seen for a single realization turned out to be much more realization sensitive and it does not seem to survive the averaging over realizations.

This work was supported by the National Science Foundation (Grant Nos. CTS-9700999 and CTS-9906794). We are grateful to E. Kierlik, G. Tarjus, and M. L. Rosinberg for ongoing discussions on the issues under study in this work.

-
- [1] For reviews see B.J. Frisken, A.J. Liu, and D.S. Cannell, *MRS Bull.* **29**, 19 (1994); M. Chan, N. Mulders, and J. Reppy, *Phys. Today* **30**, 30 (1996); L.D. Gelb, K.E. Gubbins, R. Radhakrishnan, and M. Sliwinska-Bartkowiak, *Rep. Prog. Phys.* **62**, 1573 (1999).
- [2] J.V. Maher, W.I. Goldberg, D.W. Pohl, and M. Lanz, *Phys. Rev. Lett.* **53**, 60 (1984); M.C. Goh, W.I. Goldberg, and C.M. Knobler, *ibid.* **58**, 1008 (1987); S.B. Dierker and P. Wilzius, *ibid.* **58**, 1865 (1987); S.B. Dierker, B.S. Dennis, and P. Wilzius, *J. Chem. Phys.* **92**, 1320 (1990); S. B. Dierker and P. Wilzius, *Phys. Rev. Lett.* **66**, 1185 (1991); B.J. Frisken, F. Ferri, and D.S. Cannell, *ibid.* **66**, 2754 (1991); B.J. Frisken and D.S. Cannell, *ibid.* **69**, 632 (1992); A.P.Y. Wong, S.B. Kim, W.I. Goldberg, and M.H.W. Chan, *ibid.* **70**, 954 (1993); B.J. Frisken, F. Ferri, and D.S. Cannell, *Phys. Rev. E* **51**, 5922 (1995); A.P.Y. Wong and M.H.W. Chan, *Phys. Rev. Lett.* **65**, 2567 (1990).
- [3] F. Brochard and P.G. de Gennes, *J. Phys. (France) Lett.* **44**, L785 (1983); P.G. de Gennes, *J. Phys. Chem.* **88**, 6469 (1984); A. Maritan, M.R. Swift, M. Cieplak, M.H.W. Chan, M.W. Cole, and J.R. Banavar, *Phys. Rev. Lett.* **67**, 1821 (1991).
- [4] A.J. Liu, D.J. Durian, E. Herbolzheimer, and S.A. Safran, *Phys. Rev. Lett.* **65**, 1897 (1990); A.J. Liu and G.S. Grest, *Phys. Rev. A* **44**, 7879 (1991); L. Monette, A.J. Liu, and G.S. Grest, *ibid.* **46**, 7664 (1992); J.P. Donley and A.J. Liu, *Phys. Rev. E* **55**, 539 (1997).
- [5] W.G. Madden and E.D. Glandt, *J. Stat. Phys.* **51**, 537 (1988); J.A. Given and G. Stell, *J. Chem. Phys.* **97**, 4573 (1992); C. Vega, R.D. Kaminsky, and P.A. Monson, *ibid.* **99**, 3003 (1993); E. Lomba, J.A. Given, G. Stell, J.-J. Weis, and D. Levesque, *Phys. Rev. E* **48**, 233 (1993); M.L. Rosinberg, G. Tarjus, and G. Stell, *J. Chem. Phys.* **100**, 5172 (1994); D.M. Ford and E.D. Glandt, *Phys. Rev. E* **50**, 1280 (1994); R.D. Kaminsky and P.A. Monson, *Chem. Eng. Sci.* **49**, 2967 (1994); E. Pitard, M.L. Rosinberg, G. Stell, and G. Tarjus, *Phys. Rev. Lett.* **74**, 4361 (1995); P. Bryk, O. Pizio, and S. Sokolowski, *Mol. Phys.* **95**, 311 (1998); L. Perez, S. Sokolowski, and O. Pizio, *J. Chem. Phys.* **109**, 1147 (1998).
- [6] E. Pitard, M.L. Rosinberg, and G. Tarjus, *Mol. Simul.* **17**, 399 (1996); E. Kierlik, M.L. Rosinberg, G. Tarjus, and P.A. Monson, *J. Chem. Phys.* **106**, 264 (1997); **110**, 689 (1999); M.L. Rosinberg, G. Tarjus, and E. Pitard, *Mol. Phys.* **95**, 341 (1998); E. Kierlik, M.L. Rosinberg, G. Tarjus and P.A. Monson, in *Fundamentals of Adsorption*, edited by F. Meunier (Elsevier, New York, 1998), p. 867.
- [7] J.M.D. MacElroy and K. Raghavan, *J. Chem. Phys.* **93**, 2068 (1990); J.M.D. MacElroy, *Langmuir* **9**, 2682 (1993).
- [8] R.D. Kaminsky and P.A. Monson, *J. Chem. Phys.* **95**, 2936 (1991).
- [9] K.S. Page and P.A. Monson, *Phys. Rev. E* **54**, R29 (1996); **54**, 6557 (1996).
- [10] P.A. Gordon and E.D. Glandt, *J. Chem. Phys.* **105**, 4257 (1996).
- [11] L. Sarkisov, K.S. Page, and P. A. Monson, *Fundamentals of Adsorption* (Ref. [6]), p. 847.
- [12] M. Alvarez, D. Levesque, and J.-J. Weis, *Phys. Rev. E* **60**, 5495 (1999).
- [13] F.A. Escobedo and J.J. de Pablo, *Phys. Rep.* **318**, 85 (1999).
- [14] D.A. Kofke, *J. Chem. Phys.* **98**, 4149 (1992); D.A. Kofke, *Mol. Phys.* **78**, 1331 (1993).
- [15] M.P. Allen and D.J. Tildesley, *Computer Simulation of Liquids* (Clarendon Press, Oxford, 1987).
- [16] F.A. Escobedo and J.J. de Pablo, *J. Chem. Phys.* **106**, 9858 (1997).
- [17] A.M. Ferrenberg and R.W. Swendsen, *Phys. Rev. Lett.* **61**, 2635 (1988).
- [18] W.H. Press, B.P. Flannery, S.A. Teukolsky, and W.T. Vetterling, *Numerical Recipes* (Cambridge University Press, Cambridge, 1994).
- [19] J.K. Johnson, J.A. Zollweg, and K.E. Gubbins, *Mol. Phys.* **78**, 591 (1993).